ERI_21: Diagnosis of Volcanic Activities with High-Definition Muographic Images

L. Oláh[1], G. Galgóczi[1], G. Hamar[1], O. Kamoshida[2], E.W. Llewellin[3], G. Nyitrai[1], T. Ohminato[4], S. Ohno[2], H. K. M. Tanaka[4], L. Tercsi[1], D. Varga[1]

[1]HUN-REN Wigner Research Centre for Physics,[2]NEC Corporation, [3]Durham University, [4]The University of Tokyo

I. Cosmic-ray Muography

- Passive, mass density sensitive imaging by cosmic-ray muon tracking (Fig. 1) [1].
- Shallow regions (thickness below 2-3 km) can be accessed beneath the craters.
- High (~10 m) spatial resolution can be achieved from safe (few kilometres) distance.

Figure 1: *Schematic drawing of muography and the first time-sequential muographic images [1].*

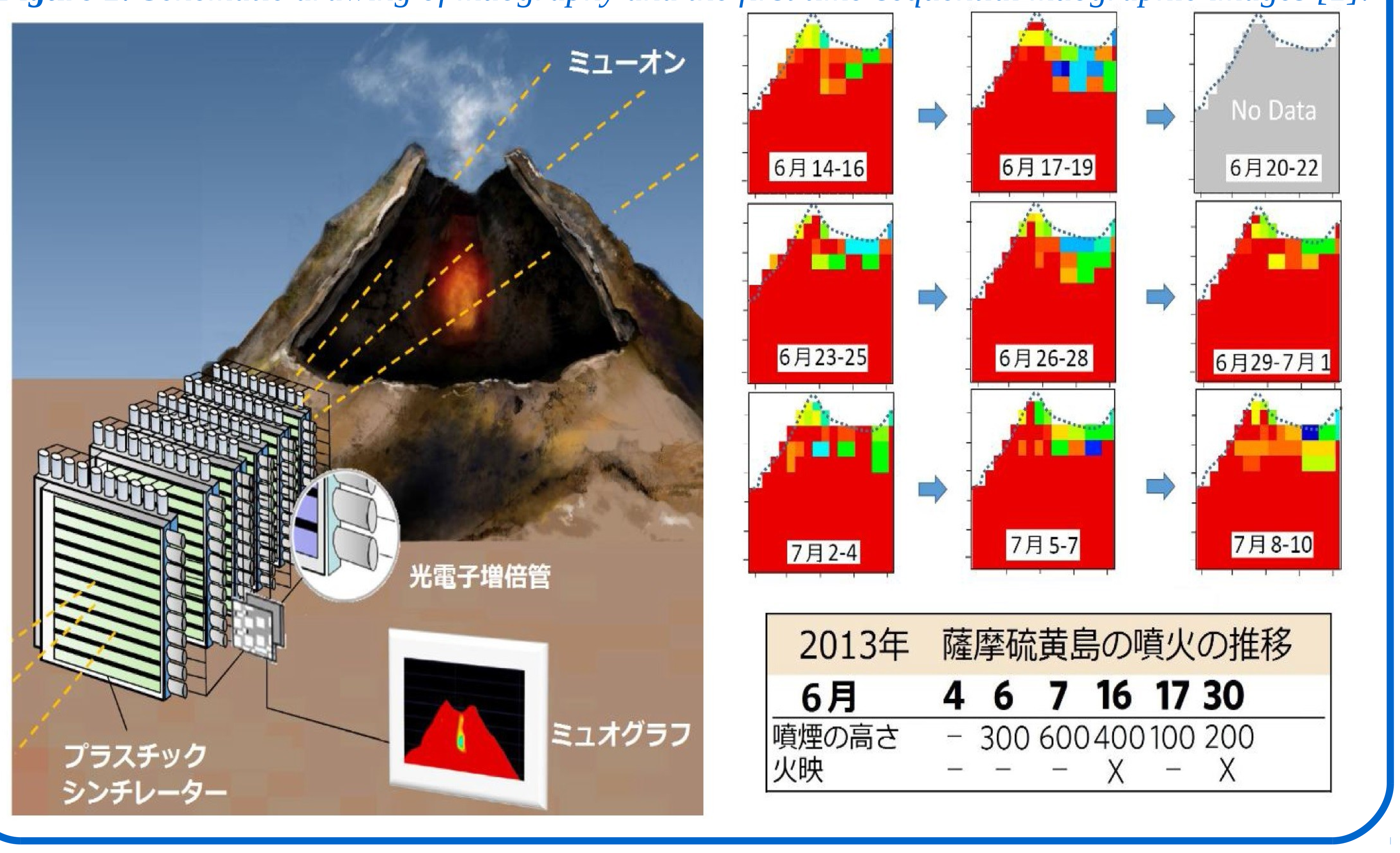

II. Sakurajima Muography Observatory

- Sakurajima is an active stratovolcano. Two craters, namely Minamidake and Showa, erupt a few hundred times per year.
- Sakurajima Muography Observatory (SMO) is continuously monitoring the flux of muons through the southern peak of the volcanic edifice from a distance of 3 km in south-west direction with an MWPC-based Muography Observation System (Fig. 2) [2,3].

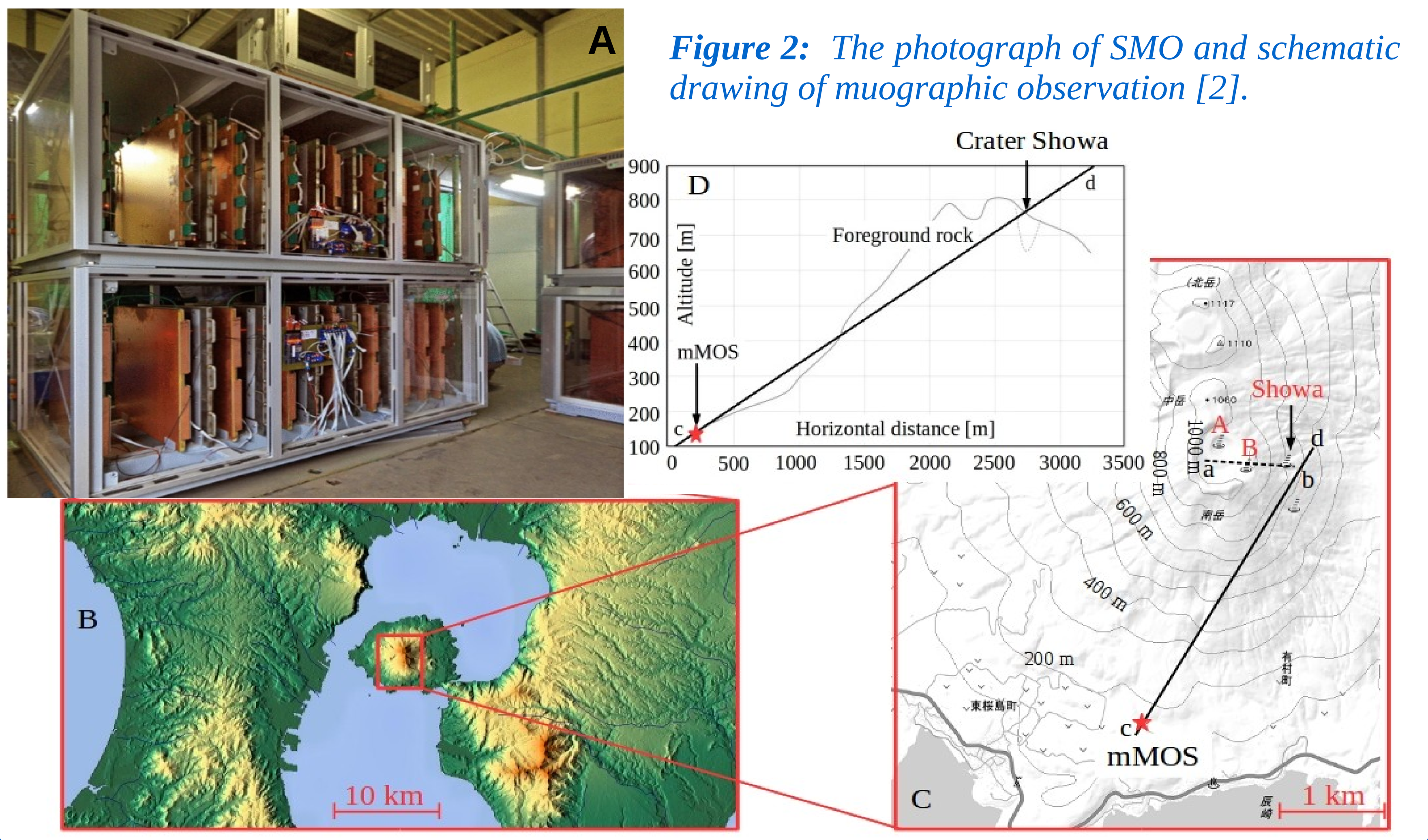

Figure 2: *The photograph of SMO and schematic drawing of muographic observation [2].*

III. Explaining Link Between Ground Deformation and Eruption Frequency

- Approximately half of ground surface deformations on volcanic edifices are followed by eruptions →Understanding the casual physical mechanism is required for interpreting the monitoring signals.
- Mass density changes reflect the change in the state of magma →Geophysical monitoring techniques (e.g., gravimetry, muography, etc.) may reveal the casual mechanism of ground surface deformations [4].
- The ground surface deformation (periodic time of 12 days) and mass density (periods of 5 months) were jointly measured at Sakurajima volcano by InSAR and muography, respectively (Fig. 3) [5].
- Periods of high eruption frequency associated with release of volcanic gases that caused the deflation of the volcanic edifice and decrease of mass density.
- Periods of low eruption frequency associated with the formation of a dense plug in the conduit, which caused inflation of the edifice by trapping pressurized magmatic gas and increase of mass density.

Figure 3: ***(A-B)*** *Muographic density images are shown without and with plug beneath the Minamidake crater, respectively [4,5].* ***(C)*** *The vertical ground deformations are, respectively, shown by blue-colored, light-blue-colored, green-colored, and yellow-colored lines at the Minamidake crater. The eruption frequency of Minamidake crater is shown by the black histogram.* ***(D)*** *The vertical uplifts are, respectively, shown by blue-colored, green-colored, and orange-colored lines at the Showa crater.* ***(E)*** *For the Reference region, the vertical uplifts are shown by blue-colored and orange-colored lines, respectively.*

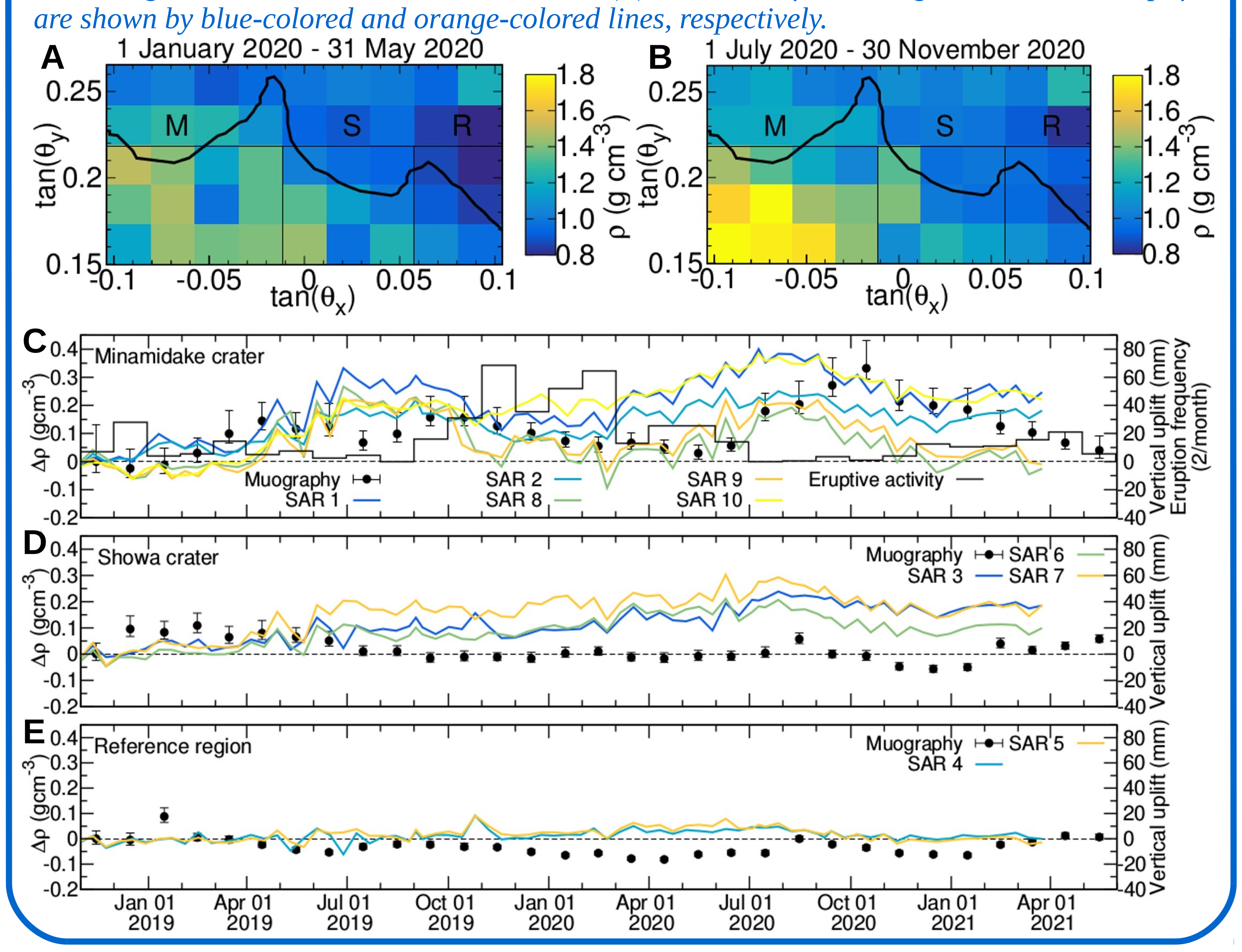

IV. Branched Conduit Structure Beneath the Active Craters Inferred from Muography

- An anti-correlation was found between the densities beneath Minamidake and Showa craters: The Pearson's coefficient was quantified to -0.52 (Fig. 4) [6].
- Inverse correlation between mass densities observed for the entire period, suggesting that magma degassing occurs either in Minamidake crater and in Showa crater, acting as a preferential pathway → a branched connection between the two conduits.
- Minamidake crater (Fig. 5A): The increasing trend in mass density is interpreted as plug formation due to magma rising. The decreasing trend is interpreted as plug reduction due to the occurrence of recurrent eruptions.
- Showa crater (Fig. 5B): Eruptions did not follow the density increase observed beneath Showa crater in January 2019 and in August 2021; however, later the mass density decreased. It was interpreted that the uprising magma generated the plug underneath Showa crater. However, the gas pressure mightn't be enough to trigger eruptions and non-solidified part of the plug drained-back.
- The InSAR and sulfur dioxide emission rate data support our current picture.

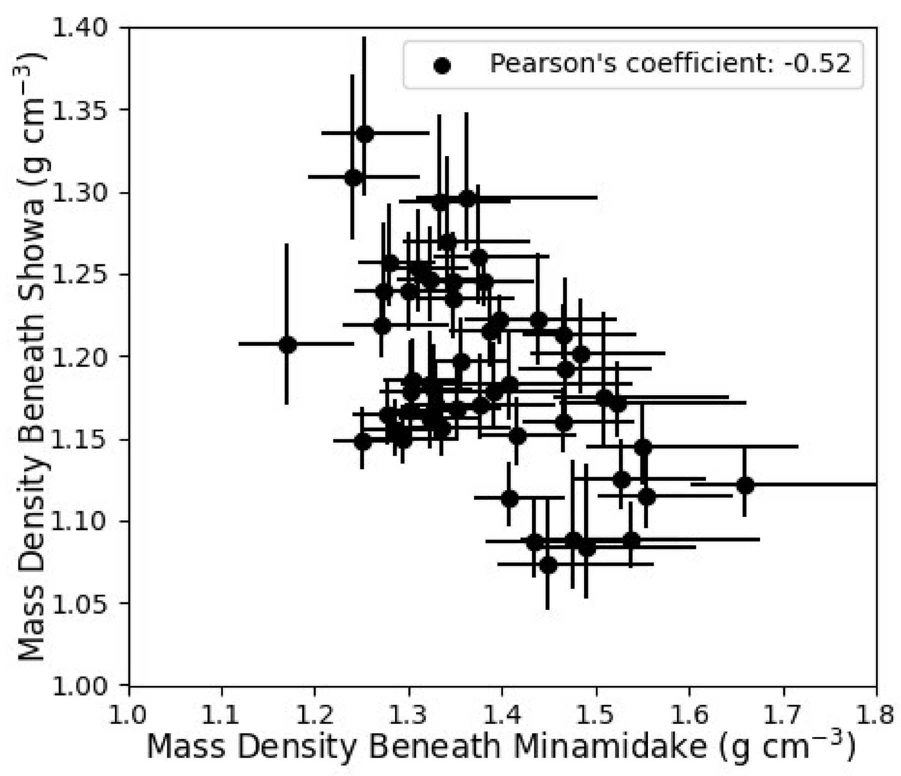

Figure 4: *Scatter plot of mass density values measured beneath the two active craters [5].*

Figure 5: ***(A)*** *Averaged densities are shown for the region beneath the Minamidake crater. The eruption frequency of Minamidake crater is shown by the orange histogram. The SO2 emission rates are shown with brown-coloured rectangles with error bars (Japan Meteorological Agency, 2022).* ***(B)*** *The average densities are shown for the region beneath the Showa crater. The eruption frequency of Showa crater is shown by the orange histogram.* ***(C)*** *Average densities are shown for the Reference region.*

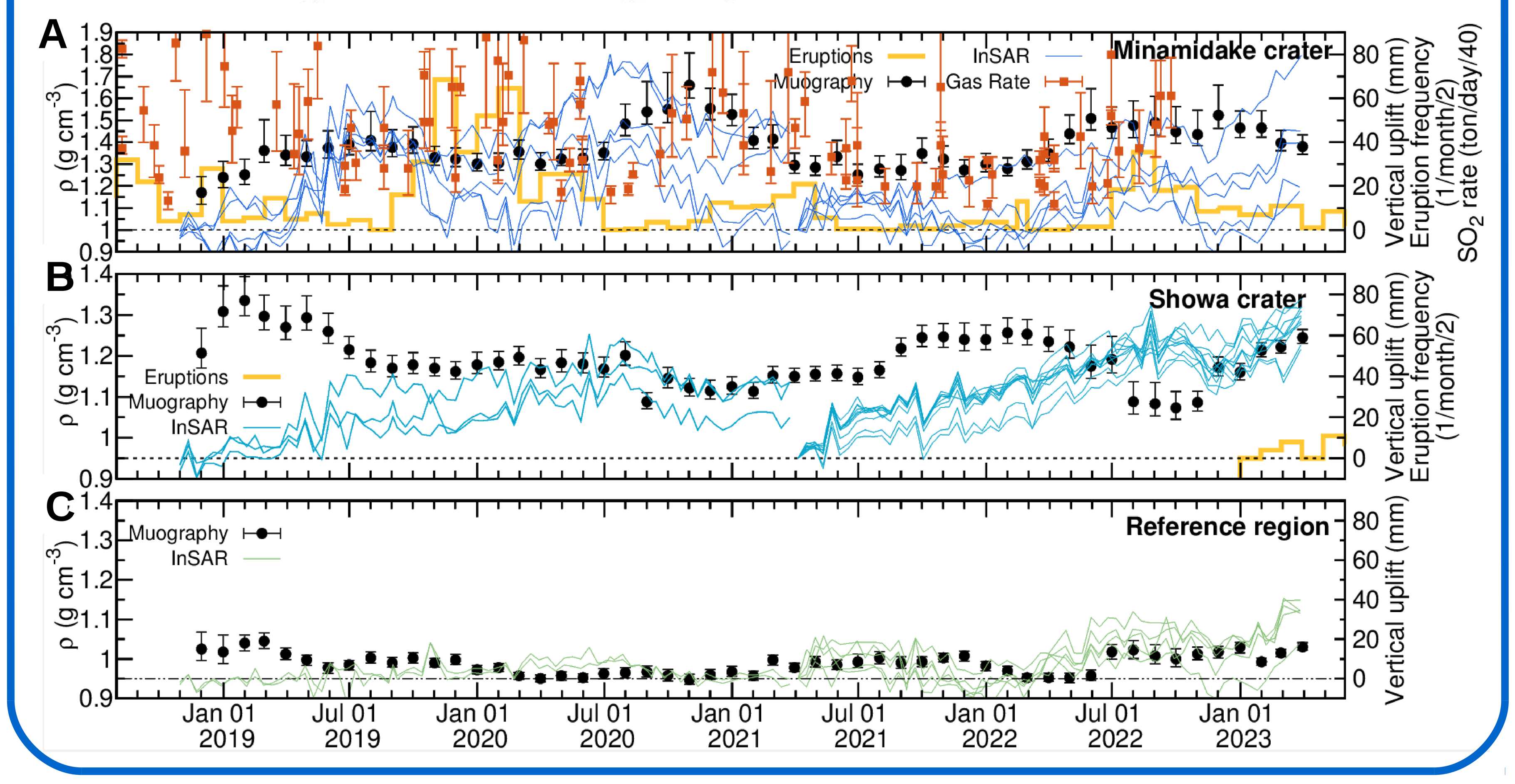

References:

[1] Tanaka, H. K. M., et al. Nat Commun 5, 3381 (2014). https://doi.org/10.1038/ncomms4381

[2] Oláh, L., et al. Sci Rep 8, 3207 (2018). https://doi.org/10.1038/s41598-018-21423-9

[3] Varga, D., et al. Nucl. Instr. Meth. A 958, 162236 (2020). https://doi.org/10.1016/j.nima.2019.05.077

[3] Oláh, L., et al. Geophys Res Lett 46, 10417-10424 (2019). https://doi.org/10.1029/2019GL084784

[4] Oláh, L., et al. Geophys Res Lett 50, e2022GL101170 (2023). https://doi.org/10.1029/2022GL101170

[5] Oláh, L. et al. Branched Conduit Structure Beneath the Active Craters of Sakurajima Volcano Inferred From Muography, manuscript under review at JGR Solid Earth (2024).

Acknowledgements:

This work was supported by the MEXT Integrated Program for the Next Generation Volcano Research, the Joint Usage Research Project (JURP) of the ERI UTokyo under project ID 2023-H-03, the Hungarian NKFIH research grants under identification numbers OTKA-FK-135349, TKP2021-NKTA-10, the HUN-REN Welcome Home and Foreign Researcher Recruitment Programme KSZF-144/2023; and the "INTENSE" H2020 MSCA RISE, GA No. 822185. Detector construction and testing was completed within the Vesztergombi Laboratory for High Energy Physics (VLAB) at HUN-REN Wigner RCP.

Corresponding Author: László Oláh (olah.laszlo@wigner.hu-ren.hu , https://wigner.hu/s/high-energy-geophysics/)